This is the Pre-Published Version.

Q. Xie, T. Gong, X. Huang (2021) *Fire Zone Diagram of Flame-Retardant Cables: Ignition and Upward Flame Spread,* **Fire Technology**. https://doi.org/10.1007/s10694-021-01133-x

Fire Zone Diagram of Flame-Retardant Cables: Ignition and Upward Flame Spread

Qiyuan Xie[1,*], Tai Gong[1], Xinyan Huang[2,*]

[1]*State Key Lab of Fire Science, University of Science and Technology of China, Hefei, Anhui, China*

[2]*Research Centre for Fire Safety Engineering, Department of Building Services Engineering, The Hong Kong Polytechnic University, Hong Kong, China*

Corresponding to xqy@ustc.edu.cn (Q. Xie); xy.huang@polyu.edu.hk (X. Huang)

Abstract: Electrical cable is a common fire risk and hazard, and once ignited, a cable fire can spread to other rooms and floors by following the direction and location of cables. This work investigated the ignition and upward flame spread over the 1-m long cable under a growing heat flux. Results showed that the flame-retardant cables could be easily ignited by a small flame after a weak irradiation (5 kW/m^2) if preheated to 70 ℃. As the external radiation increases, the cable surface temperature increases, and the upward flame spread rate increases significantly. Once the cable surface reaches 240 ℃, piloted ignition can be achieved. With the combined effect of external heating (>18 kW/m^2) and smoldering, auto-ignition could be achieved once the cable sheath reaches 500 ℃. Moreover, flame-retardant cable fire is intense with severe melting, dripping, swelling, and cracking. The falling cracks and dripping flow can form a pool fire to increase the fire hazard. Finally, a new fire-zone diagram with the surface temperature and critical mass flux was proposed to quantify the cable fire hazard. This work provides important information about fire behaviors of the flame-retardant cable under a real fire scene and may guide the design of fire-resistant cables.

Keywords: *transient heat flux; PVC/PE cable; fire spread; growing fire heating; fire hazard mapping*

Graphic Abstract

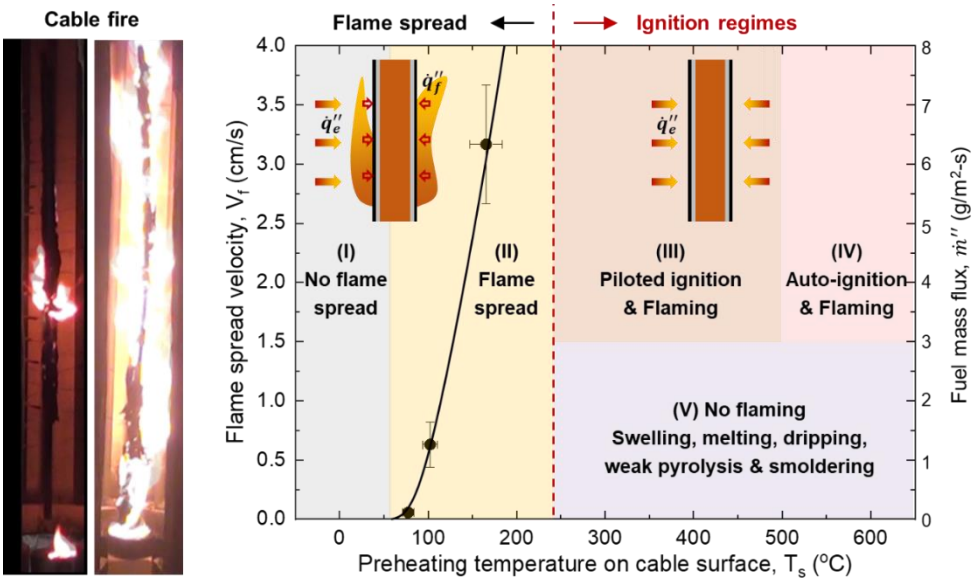

1. Introduction

Electrical cables with polymer insulation have been considered as a possible source and typical load of fire in residential buildings, factories, nuclear power plants, aircraft, and space vehicles [1–3]. That is because electrical cables can be ignited due to short circuits, poor contact, ground fault, and external heating [4]. Fundamentally, what makes the combustion phenomenon in cable fire unique is its default combination of the outer sheath, polymer insulation, and the inert metal core [2]. The fact that the thermal conductivity of the metal core is 2-3 orders of magnitude greater than the polymer insulation or sheath can significantly alter the heat transfer in the ignition and spread of cable fire. Today, flame-retardant cables were used more widely under the new safety requirement of fire codes and regulations, particularly in new high-rise buildings, underground spaces, nuclear power plants [5], data centers, and telecommunication rooms. These flame-retardant cables are not incombustible in nature. Moreover, they have complex fire behaviors during ignition and burning, such as auto-ignition, swelling, cracking [6], melting and dripping [7–9], which need a better scientific understanding.

In the literature, most fundamental studies focused on the fire behaviors of thin wire samples (diameter < 10 mm), e.g. [10–13], which were made of a metal rod as the core and a single layer of insulation. For those thin wires, the decomposition of insulation and the heat transfer in the radial was often fast enough to be ignored. However, commercial cables normally have multiple metal cores and several layers of thick flame-retardant polymer layers [3,14–18], so that the heat transfer, deformation, phase change, and decomposition chemistry become crucial to fire behaviors. Babrauskas *et al.* [3] in the early 90s reviewed the fire performance of wire and cables and the standard tests for cable fire in different countries. Tewarson and Khan [14] tested the upward flame spread over 35 commercial electrical cables with a copper or aluminum core, and found the metal core acted as the heat sink to slow down the flame spread. More recently, Journeaux *et al.* [15] and Huang *et al.* [16] studied the upward fire spread over vertical cable trays with multiple cables and quantified the fire-spread rate without external radiation.

The existence of external heat flux is a key characteristic of a real fire scene that controls ignition and flame spread behavior of cable and other fuels [19–21]. To understand the ignition criteria, most past works used a constant external heat flux [2,22–24]. Fernandez-Pello *et al.* [19] studied the pilot-ignition time and the flame-spread rate of several commercial cables under a range of external radiations and showed that the ignition temperature of cable was similar to the pyrolysis temperature of cable insulation. However, in most real fire scenarios, materials are ignited usually under an increasing external heat flux, rather than a constant heat flux. In the pre-flashover (or growth) stage, with the increase of fire size and intensity, the material is more likely to be heated and eventually ignite under an increasing heat flux. Because of its complexity, very few studies have looked into the ignition behavior under a transient heat flux [6,25–27]. Vermesi *et al.* [25,26] studied the piloted and spontaneous ignition processes of plastic and wood under the transient (or time-dependent) external radiation. They revealed that traditional ignition criteria for constant heat flux became inappropriate.

In the previous work [6], the swelling and auto-ignition behavior of 0.1-m long flame-retardant cable were experimentally studied based on a novel facility with external radiation up to 90 kW/m^2. We found the observed spontaneous ignition was a unique outcome of pyrolysis gas that was released from inner XLPE insulation, piloted by the smoldering hot spot on the outer swelling and charring PVC sheath. Such spontaneous ignition occurred when the cable surface temperature exceeded 500 ℃. In this work, we further investigated the upward flame spread over the 1-m long flame-retardant cable in a semi-real fire scenario, where the cable was ignited by a flame under the growing external heat flux.

2. Experimental Methods

2.1. Cable samples

Fig. 1 shows the 1-m long commercial flame-retardant cable (ZR-YJV) tested in this work, which was the same as the 0.1-m cable sample in our previous research [6] and similar to the (PVC/PE coaxial cable) used in [19]. The cable had three layers, namely, the polyvinyl chloride (PVC) sheath layer, the cross-linked polyethylene (XLPE) insulation layer, and the inner bunch of copper cores. The diameter of the whole cable sample was 22 mm, while the one for the inner copper core was 16 mm. The thicknesses of PVC sheath layer and XLPE insulation layer were 1.6 mm and 1.4 mm, respectively. More information about the cable sample and experimental facility can be seen in [6].

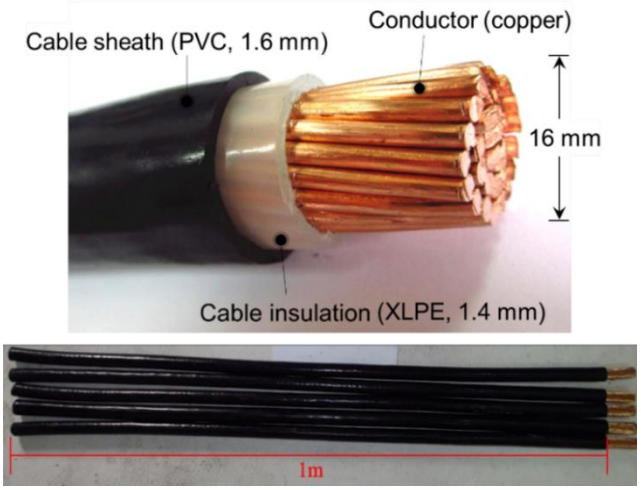

Fig. 1. Photos of the 1-m long flame-retardant cable sample with detailed structures and dimensions.

2.2. Experimental setup

Fig. 2 shows the (a) schematics and (b) photo of the test facility for ignition and spread of cable fire that was the same as the previous work [6] and similar to that in [19]. The setup included three main parts, namely, a cylindrical fire chamber with controllable external heat fluxes [6], a frame for holding the cable sample vertically, and the data measurement system. The wall of the heating chamber was made of Mullite bricks and covered by the outer steel shell to ensure excellent heat insulation and structural stability. Eighteen electric heating rods of 120 cm length were placed equidistantly around the inner wall of the chamber. This chamber introduced a uniform annular heat flux for the cable sample

on the centerline, which was different from the singe-side gas-fired radiant panel in [19]. The heating and fire behaviors of cable samples were monitored by a CCD camera (50 fps) through a narrow gap in the chamber (see a top view of Fig. 2a).

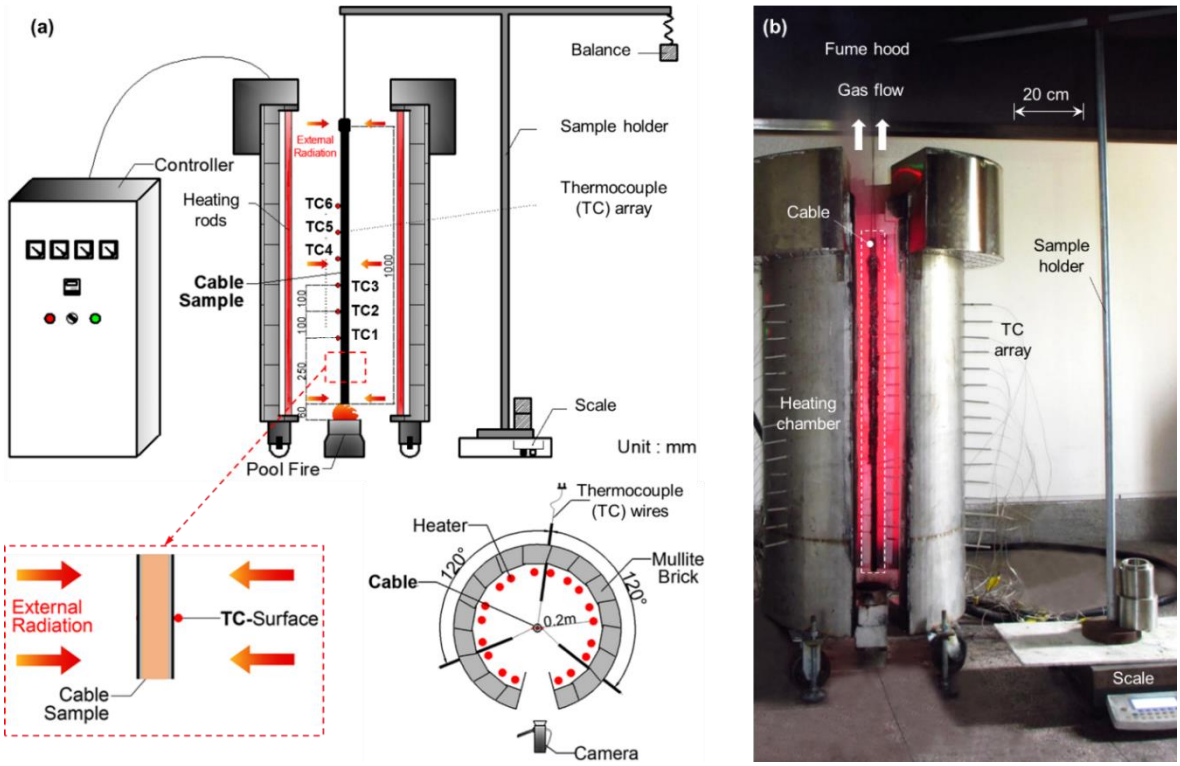

Fig. 2. (a) Schematic of the facility for ignition and flame spread of the vertical cable with varying annular heating flux, and (b) photo of the test facility.

During the tests, the temperature profile of cable along the cable sample was monitored by 6 thermocouples (Type K with a 0.5-mm bead). These thermocouples only gently touched the cable surface, which minimized the influence on the sample mass measurement. The vertical distance between the adjacent thermocouples was 100 mm, with the lowest one 250 mm from the bottom of the cable. The thermocouple data were also used to quantify the flame spread rate, that is, the flame leading edge was defined when the thermocouple exceeded the fuel pyrolysis temperature (250 °C) [28]. Note that in experiments, due to the swelling and cracking of the cable coating, its contact with thermocouple beads might provide accurate temperature data after flame spread over.

2.3. Transient external heat flux

The radiant heat flux at the middle of the fire chamber centerline was controlled by the power of 18 heating rods. Once turning on the power, the heating rods would gradually increase the temperature due to the large thermal inertia. As a result, the heat flux around the cable sample also increased gradually, which mimicked the environmental heating of a real fire scene in the growth stage. Moreover, the relatively slow heating process at the beginning ensured the heating of the inner metal core and minimized the temperature difference in the cross-section of the core before ignition.

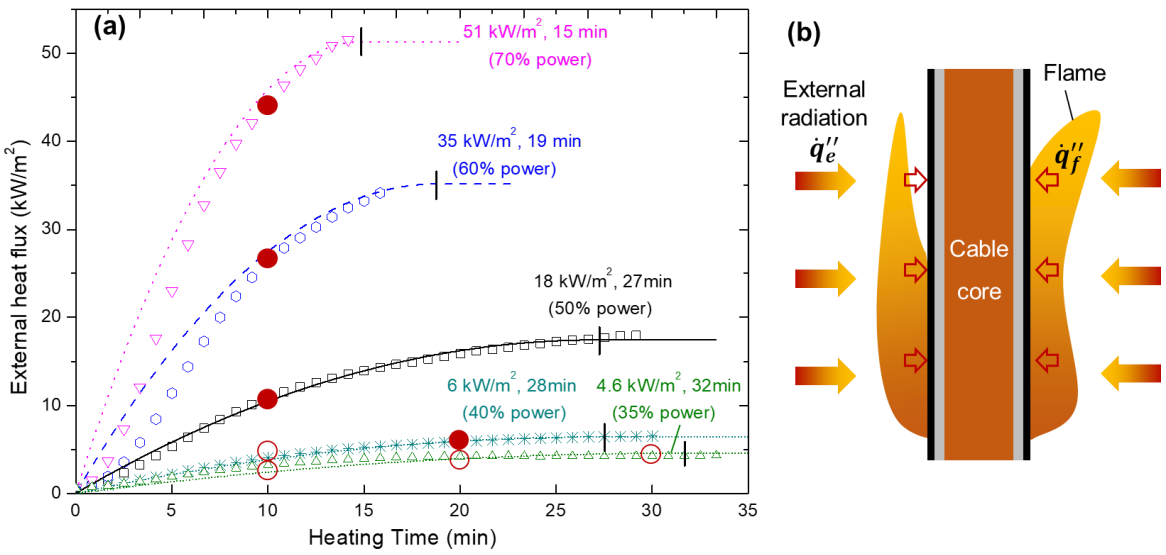

Fig. 3. (a) Transient heat flux in the vertical centerline under 5 heating power, where hollow symbols are experimental measurements, lines are the t^2 fitting curves, ● and ○ indicate a successful and failed piloted ignition, respectively, and (b) diagram for cable which is heated by both the flame ($\dot{q}_f''$) and external radiation ($\dot{q}_e''$).

Fig. 3 shows the measured transient heat flux profiles under five heating powers, from 35% to 80% of the full heating power (i.e., 5 kW × 18 = 90 kW). The heat flux increased faster at a higher heating power when a higher voltage was set for heating rods. The transient external heat flux, $\dot{q}_e''(t)$ [kW/m^2], in the fire chamber can be well described by the t^2 model as

$$\dot{q}_e''(t) = \begin{cases} -a \cdot (t - t_m)^2 + \dot{q}_{max}'' & (t < t_m) \\ \dot{q}_{max}'' & (t \geq t_m) \end{cases} \quad (1)$$

where $a = \dot{q}_{\max}''/t_m^2$ is the growth coefficient, $\dot{q}_{\max}''$ is the maximum heat flux [kW/m^2] at the final steady heating state, and t_m is the time [s] needed for reaching the steady heating state.

Table 1. Parameters of t^2 growth fitting for the five increasing heating scenarios in the fire chamber

Heating Level (% of Full Power)	$\dot{q}_{\max}''$ (kW/m^2)	t_m (s)	a (kW/(m^{2}s^2))
35%	4.5	1900	1.2×10^{-6}
40%	6	1670	2.3×10^{-6}
50%	18	1630	6.7×10^{-6}
55%	28	1370	1.6×10^{-5}
60%	35	1130	2.7×10^{-5}
70%	51	890	6.4×10^{-5}
80%	61	540	3.6×10^{-4}

Therefore, two parameters ($\dot{q}''_{\max}$ and t_m) were sufficient to fully describe the external heat flux. Table 1 lists the fitting parameters for these five heating conditions. A higher heating power results in a faster heat flux increase and a larger maximum heat flux. For example, under the 70% heating level, it took about t_m = 15 min to reach the maximum heat flux of about $\dot{q}''_{\max}$ = 51 kW/m^2, while it took t_m = 28 min to reach $\dot{q}''_{\max}$ = 6 kW/m^2 under the 40% heating level.

2.4. Fire test protocols

Before each test, the cable sample was hung vertically in the centerline of the chamber using a T-shape frame. The sample frame was placed on the scale with a mass balance (see Fig. 1). The cable sample was first preheated by the growing annular heat flux, and then, a small pool fire was placed 5-cm below the bottom of the cable as the ignition source for both heating and piloting (similar to [19]). The pool fire had 50-mL heptane in the pan, and it provided a 10-kW flame the bottom of cable for about 5 min. As the level of external radiation increased, the HRR of pool fire increased, and its burning duration decreased.

The preheating time was first set to 10 min, and if piloted ignition was not achieved, a longer preheating time (20 or 30 min) was used for a new sample. Table 2 summarizes all experimental cases with different preheating powers and durations. For each condition, at least 3 repeating tests were conducted, and a good experimental repeatability was shown.

Table 2. Cases and qualitative results of ignition and flame spread of 1-m flame-retardant cable by pilot flame ignition after preheating for a certain period.

Percentage of full heating Power ($\dot{q}''_{\max}$, t_m)	Preheating time (min)	Outcome of pilot-ignition with flame	Flame spread rate (cm/s)	Outcome of auto-ignition [6]
35% P_{max} (4.5 kW/m^2, 32 min)	10	No ignition	-	No ignition
	20	No ignition	-	No ignition
	30	No ignition	-	No ignition
40% P_{max} (6 kW/m^2, 28 min)	10	No ignition	-	No ignition
	20	Bottom ignition & flame spread	0.06±0.02	No ignition
50% P_{max} (18 kW/m^2, 27 min)	10	Bottom ignition & flame spread	0.63±0.19	No ignition
55% P_{max} (18 kW/m^2, 27 min)	10	Bottom ignition & flame spread	3.2±0.5	Auto-ignition (≈ 16 min)
60% P_{max} (35 kW/m^2, 19 min)	10	Ignition of whole cable (flame propagation)	>100	Auto-ignition (≈ 11 min)
70% P_{max} (51 kW/m^2, 15 min)	10	Ignition of whole cable (flame propagation)	>100	Auto-ignition (≈ 8 min)
80% P_{max} (51 kW/m^2, 15 min)	10	Ignition of whole cable (flame propagation)	>100	Auto-ignition (≈ 6 min)

3. Results and Discussions

3.1. Limit for cable ignition and upward flame spread

Table 2 and Fig. 3a summarize the experimental outcome of the piloted ignition under external radiation and compare with the auto-ignition results in the previous work [6]. At the 35% heating power (up to 4.5 kW/m^2 within 32 min), the piloted ignition and upward flame spread could not be achieved, even after a preheating time of 30 min and the burnout of pool fire for another 5 min (see Fig. 4 and Video S1). After the burnout of pool fire, only the bottom part of cable was partially burnt, while the flame could not maintain on the cable. Increasing to 40% heating power (up to 6 kW/m^2 within 28 min), a 10-min preheating time plus a 5-min poor fire still could not achieve the fire spread, when the external heat flux reached about 4 kW/m^2. Nevertheless, if extending the preheating time to 20 min and reaching the external heat flux of 6 kW/m^2 or further increasing the heating power, ignition and upward fire spread would be successful. Therefore, we can conclude that the minimum external heat flux to ensure the upward flame spread over this cable is 5.5 ±0.5 kW/m^2.

Note that the external heat flux here mimicked environmental heating in addition to the flame heat flux from the bottom pool fire or the ignited cable fire (Fig. 3b). It is different from the external radiation in a conventional cone-calorimeter test with a spark pilot [29]. To achieve a conventional piloted ignition under external radiation, a minimum heat flux of 25-28 kW/m^2 was needed for a similar 22-mm PVC/PE cable [19]. On the other hand, the auto-ignition of this cable can be achieved when the external heat flux exceeds 18 kW/m^2, or the PVC sheath surface temperature exceeds 500 °C (see more details in Ref. [6]). For both the convectional piloted ignition and auto-ignition, the whole cable will be ignited simultaneously (i.e., gas-fuel flame propagation), so there is not any fire-spread process, as discussed more in later sections.

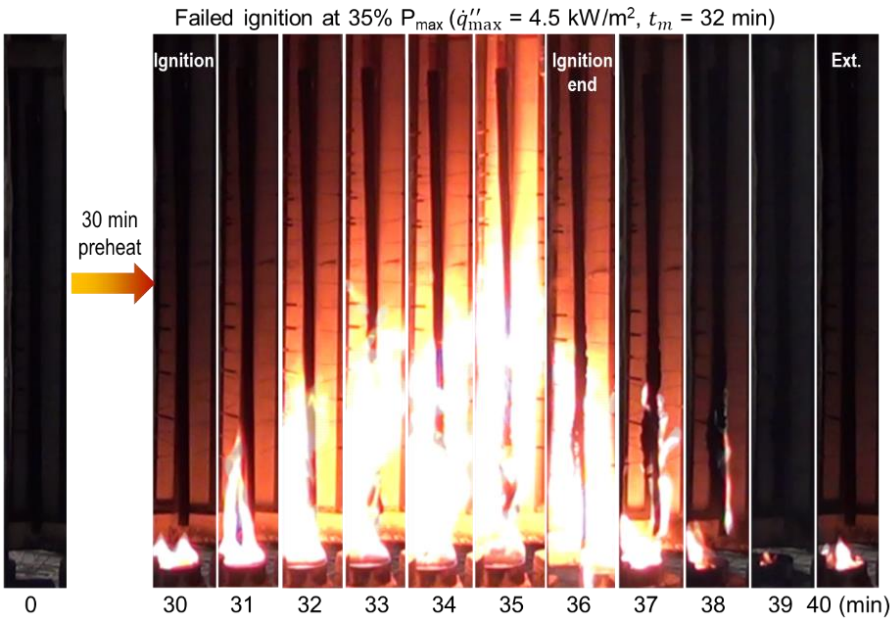

Fig. 4. Snapshot series of failed ignition of the cable under the external heat flux of 35% P_{max} ($\dot{q}''_{max} = 4.5$ kW/m^2, $t_m = 32$ min) with 30 min preheating (Video S1).

3.2. Cable ignition and fire spread under weak irradiation

Fig. 5 show the series of photos for the ignition and upward flame spread of vertical cable sample after two external heating conditions, where time zero is moment of turning on the heater. Fig. 6 shows the corresponding surface temperature data. For the 40% heating power (up to 6 kW/m^2 within 28 min) in Fig. 5a and Video S2, during the 20 min preheating, there was no obvious swelling and other shape change of the cable, because the surface temperature barely reached 70 ℃ (see Fig. 6a).

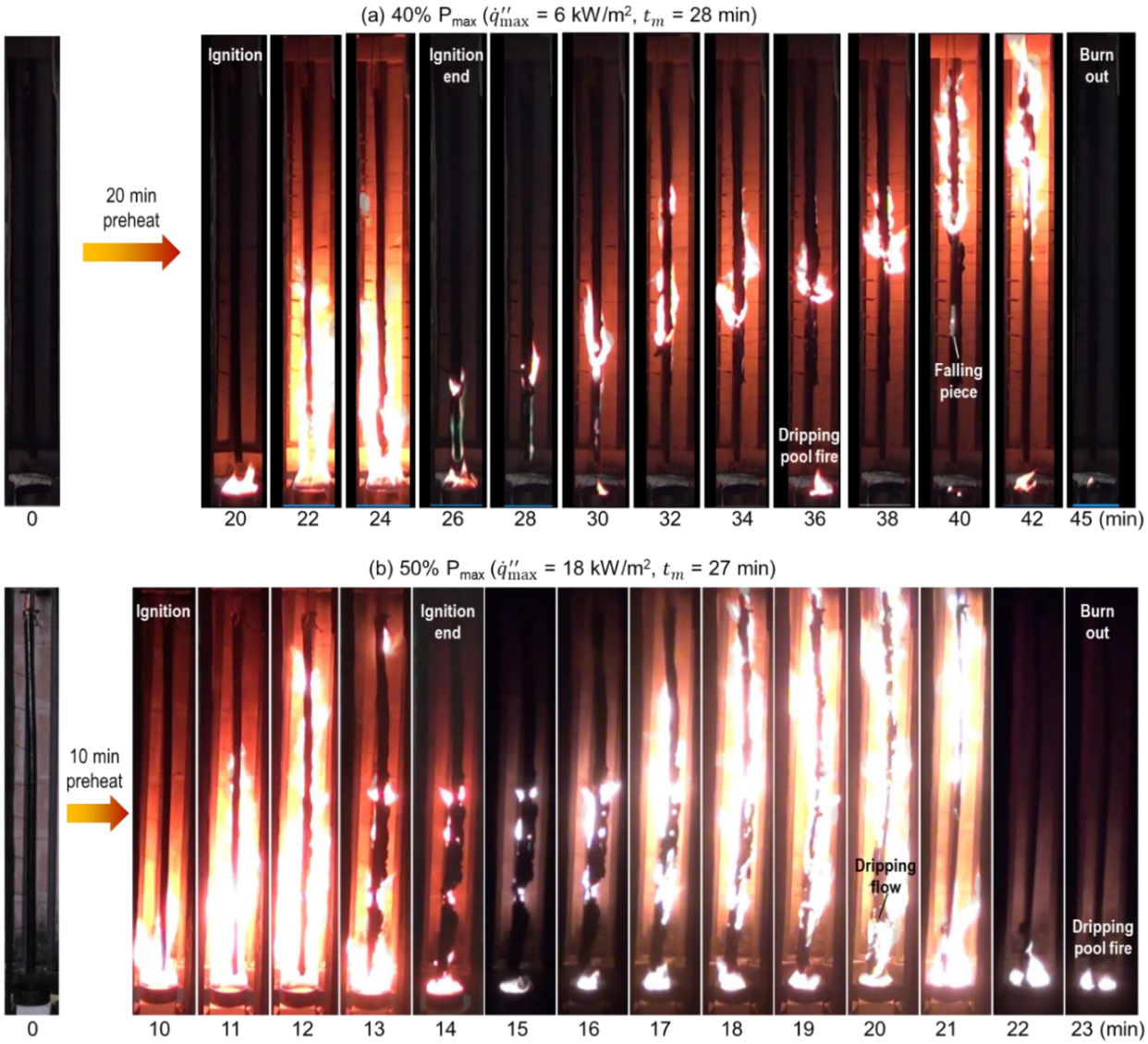

Fig. 5. Snapshot for ignition and upward fire spread of cable under a weak external radiation, (a) 40% P_{max} ($\dot{q}''_{max}$ = 6 kW/m^2, t_m = 28 min) with 20 min preheating (Video S2), and (b) 50% P_{max} ($\dot{q}''_{max}$ = 18 kW/m^2, t_m = 27 min) with 10 min preheating (Video S3).

Once the pool fire was initiated on the bottom, the flame height gradually increased, because part of the cable was ignited and contributed to the flame. Such initial upward flame motion could be considered as the pool-fire assisted flame spread. By the time that the pool was burnt out (at 24 min), the flame could reach the height of about 40 cm, but only less than 20 cm near the bottom was truly

ignited. Afterward, the cable fire started to spread upward, and the size of flame was small, as discrete peaks can be found in the thermocouple measurements (Fig. 6a), during which the size of the flame and burning zone grew slowly. Eventually, it further took 15 min for the small flame to spread to the top, and then another 5 min to burn out the entire cable.

Note that a pool fire reappeared in the pan during the upward flame spread (see Fig. 5). That was a pool of molten PE insulation layer that formed a dripping flow from the cable core to the pool. Such a downward dripping flow (also called as flooring [8]) contributed to the increasing burning region during the upward flame spread. Near burnout, the PVC sheath layer of the cable broke into large pieces and fell with a flame, which could cause a significant fire hazard.

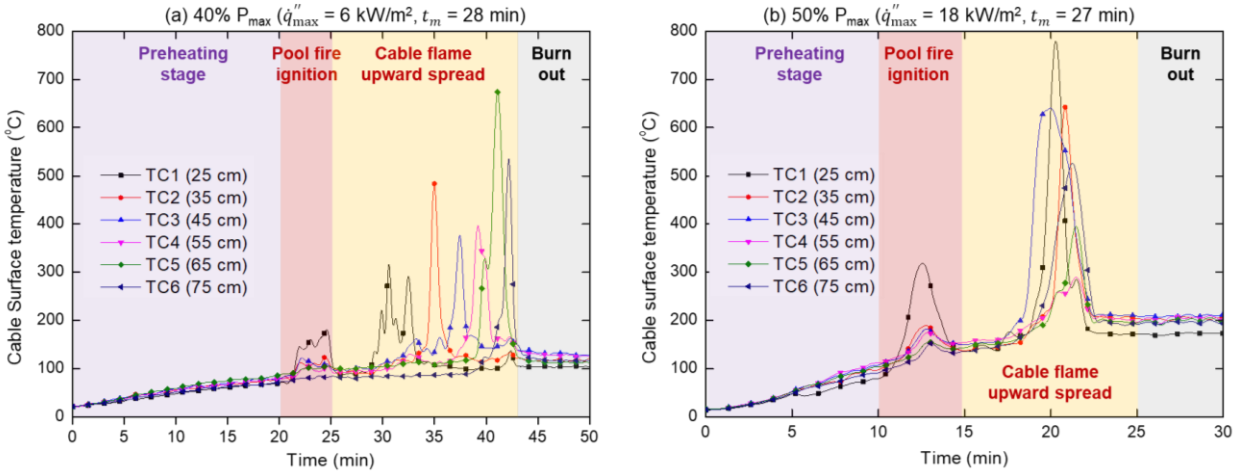

Fig. 6. Cable surface temperature evolution under a weak external heat flux, (a) 40% $P_{\max}$ ($\dot{q}''_{\max} = 6$ kW/m^2, $t_m = 28$ min) with 20 min preheating, and (b) 50% $P_{\max}$ ($\dot{q}''_{\max} = 18$ kW/m^2, $t_m = 27$ min) with 10 min preheating.

Increasing the heating power to 50% (up to 18 kW/m^2 within 27 min) and preheating for 10 min, the cable surface temperature reached about 100 ℃ (Fig. 6b). In this case, the cable was ignited more easily with a stronger flame, and the bottom pool-fire flame could quickly cover the entire cable, as shown in Fig. 5b and Video S3. After the burnout of the heptane pool fire (at 14 min), about half of the cable was ignited, despite that the flame on cable was still relatively weak. More importantly, the cable swelled, broke into several pieces, and peeled off after the intense heating from both the pool fire and external radiation. Afterward, the cable surface temperature continued to increase, and the flame quickly re-developed, where it quickly spread both upward and downward to cover the entire cable within 3 min. Compared to 40% power in Fig. 5a, the burning region was much longer in Fig. 5b, as indicated by the overlapping temperature curves in Fig. 6b.

Compared with the initial burning assisted by the pool fire, the later spread and burning stage was even stronger, and the cable was burnt out within another 3 min. Note that the continuous dripping of molten PE sustained a robust pool fire during the flame spread and after the burnout of cable. Because of stronger heating from both cable flame and external radiation, such an intense dripping and falling

of cable coating was also expected. These tests demonstrate that as long as a small external radiation (up to 6 kW/m^2) is present to slightly heat up the cable coating to about ~70 °C, the conventional flame-retardant cable can be easily ignited by a small flame. Considering a typical sprinkler activates at about 65 °C, this "flame-retardant" cable could be ignited in the early stage of a compartment fire. Moreover, the vertical flame-retardant cable can easily support the flame spread from the floor to ceiling or higher floors like the curtain in a real fire scenario. Thus, it could pose a significant fire hazard.

3.3. Cable ignition and burning under strong irradiation

Fig. 7a shows the photos of the cable ignition and burning process under the 60% heating power (up to 35 kW/m^2 within 19 min) and see more details in Video S4. After preheating for 10 min, the external heat flux was about 26 kW/m^2, and cable surface temperature exceeded 180 °C (see Fig. 8a), which was close to the pyrolysis temperature of the PVC sheath (see TGA in Ref. [6]). Moreover, the PVC sheath layer of the cable sample swelled and cracked significantly, and similar behaviors were also observed for the 0.1-m cable sample previously [6]. It was also close to the minimum heat flux of 28 kW/m^2 for piloted ignition found in the single-side radiant panel test [19]. Therefore, once the pool fire was present, the flame quickly spread up over the entire cable within 1 s, where the observed flame speed was 192 cm/s. Thus, it was the propagation of premixed flame on the mixed heptane vapor (heptane boiling point of 98 °C) and cable pyrolysis gases. As heated by the flame, the surface temperature of cable quickly increased above its ignition point, so that both the heptane pool and the cable were burning severely. After another 5 min, the half-burnt cable sheath and insulation fell and continued to burn the ground.

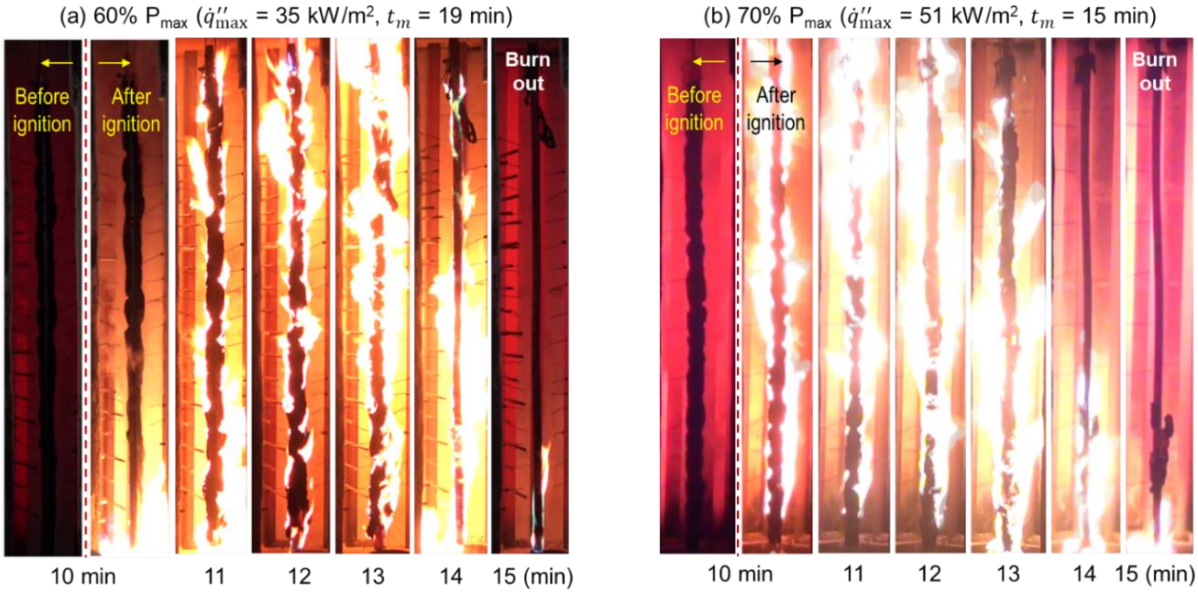

Fig. 7. Snapshots for cable ignition process under a strong external heat flux with 10 min preheating, (a) 60% P_{max} ($\dot{q}''_{max}$ = 35 kW/m^2, t_m = 19 min) and see Video S4, and (b) 70% P_{max} ($\dot{q}''_{max}$ = 51 kW/m^2, t_m = 15 min) and see Video S5.

Fig. 7b shows the photos of the cable ignition and burning process under the 70% heating power (up to 51 kW/m^2 within 15 min) and see more details in Video S5. After preheating for 6 min, the external heat flux had reached about 30 kW/m^2, and an intense smoke plume was observed within the heating chamber. Also, the PVC sheath was heated above 250 ℃ (see Fig. 8b), which was higher than its pyrolysis point, as well as the threshold temperature of char oxidation (see TGA curves in Ref. [6]). Thus, the smoldering ignition of PVC was first achieved, which accelerated the temperature increase through the heterogeneous exothermic oxidation [30], as shown in the smoldering region in Fig. 8b. By the end of the 10 min preheating, the smoldering of PVC also led to severe swelling and cracking, and increased its temperature above 500 ℃, which would achieve auto-ignition even without the pilot source [6]. Once the pool fire was present, the whole cable sample was ignited immediately with a flame propagation speed >100 cm/s. Because of the intensive flame and external radiation, much more melting and dripping of PE flow down, as well as the cracking pieces of the PVC layer. Shortly after, the entire remaining PVC sheath fell and continued burning on the ground.

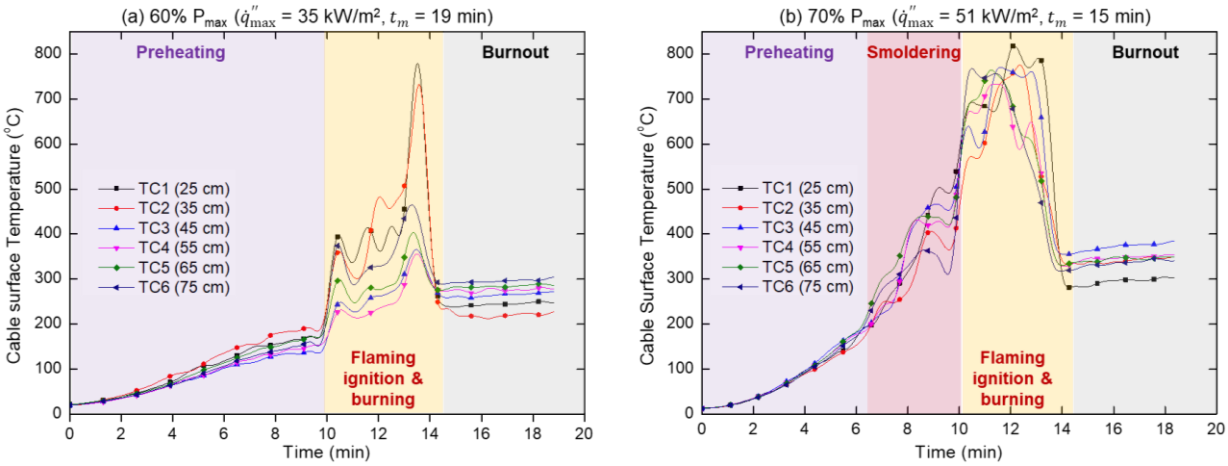

Fig. 8. Cable surface temperature evolution under a strong external heat flux with 10 min preheating, (a) 60% $P_{\max}$ ($\dot{q}''_{\max} = 35$ kW/m^2, $t_m = 19$ min), and (b) 70% $P_{\max}$ ($\dot{q}''_{\max} = 51$ kW/m^2, $t_m = 15$ min).

3.4. Cable fire zone diagram

To quantify the flammability of material, the convectional heat-flux-based diagram (such as the cone calorimeter [31] and LIFT test diagram [32,33]) are often used. The LIFT (Lateral Ignition and Flame-spread Test) diagram combines the data of two separated tests (1) the piloted ignition test and (2) flame spread test, into one diagram, which share the same x-axis of surface temperature while two y-axes (flame spread rate and piloted ignition time) are different. However, to further quantify the fire zones of cable, the convectional heat-flux-based diagram become inappropriate for two reasons:

(1) The external heat flux is not necessary a constant but time-dependent, especially in real fire scenarios, so that it is difficult to use a single parameter to quantify the external heat flux.

(2) In addition to external heat flux, most real cable sheath and insulation layers can be charred and self-heated by the smoldering process. For example, the cable can be auto-ignited in a relatively

low external radiation (as low as 18 kW/m^2 [6]), making the convectional heat-flux-based criteria no longer valid.

Therefore, as an analogy to the classical LIFT diagram, we proposed a new **fire-zone diagram** with both the fuel surface temperature and the critical mass flux of ignition, and it is only related to the fuel characteristics while independent of external heating conditions.

Fig. 9 summarized the zones for different cable fire behaviors as a function of preheated cable surface temperature, where the flame-spread part is based on this work, and the ignition part is based on previous work [6]. For this PVC/XLPE, if there is no preheating or the preheated surface temperature is less than 70 °C (external heat flux < 5 kW/m^2), the cable cannot be ignited by a localized pool fire on the ground to support an upward fire spread (Zone I). Further preheating the cable surface above 70 °C, the flame spread can be sustained, and the rate of spread increases significantly with the surface temperature (Zone II). Specifically, with preheating to 70 °C, the flame spread is slow, only 0.06 cm/s, and spreading up for 1 m needs almost 20 min (Fig. 5a). Once preheated to 170 °C, the flame spread rate increase 50 times to 3.2 cm/s. Note that if the ignition source is strong and can continuously increase the fuel surface temperature, eventually the flame spread becomes possible, as seen from this diagram.

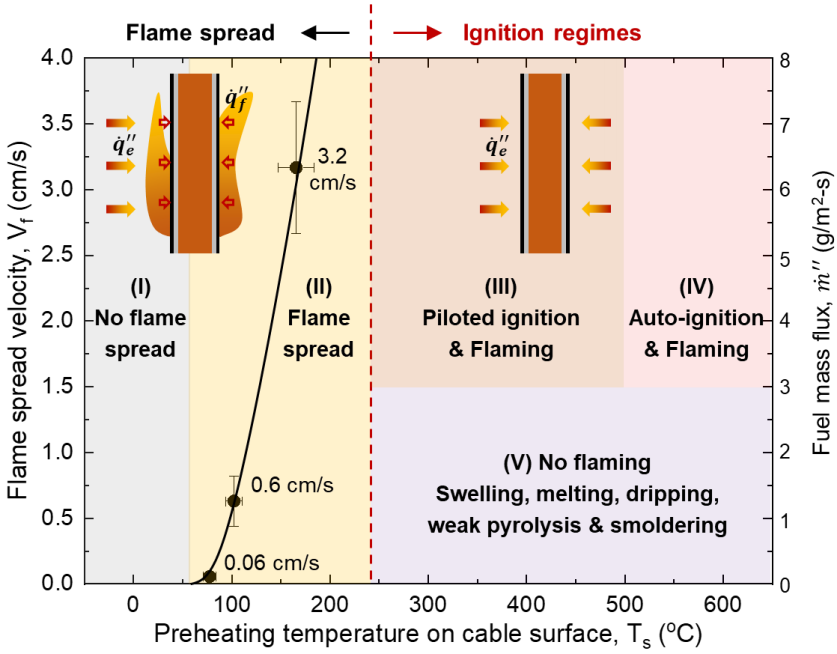

Fig. 9. Cable fire-zone diagram with ignition and fire behaviors as a function of surface temperature, where Zones (I) no flame spread, (II) flame spread, (III) piloted flaming ignition, (IV) auto flaming ignition, and (V) no flaming.

Once preheating the cable above 240 °C (about the pyrolysis temperature of PVC sheath), a small pilot flame or spark can achieve the piloted ignition and the flame can quickly cover the entire cable like the flashover (Zone III), and the observed flame "spread" is essentially the premixed flame propagation. Further preheating the cable above 500 °C, the pilot source is no longer needed, instead, an auto-ignition and the flaming of entire cable can be achieved (Zone IV). Because the cracked surface is

smoldering intensively and the glowing hot spots (above 700 ℃) can act as the piloted source, only a medium level external heat flux (18 kW/m^2) is required for auto-ignition [6], which is different from other non-charring plastic materials. Note that commercial cable is a thick material, and the metal core is an excellent heat sink [2].

To achieve either piloted ignition or auto-ignition, a minimum fuel mass flux of 3 g/m^2-s is required. Below this limit (Zone V), no flaming ignition is observed. Instead, only slow pyrolysis and smoldering of the outer PVC layer exist, which also has complex swelling and cracking process before breaking into pieces. Before that, the inner PE layer has already melted and dripped away, and the copper core continues to cool the inner boundary of PVC layer and minimize the mass flux. As a result, ignition is never achieved, as observed for the 10-cm sample in the Part-I [6].

Note that like all other fire test, the presented data and diagram depend on the apparatus, similar to all other fire tests, so care is needed when referring this diagram for other tests and fuels. Also, the cable is a complex fuel, and its flammability may not be quantified by a simple parameter, such as the critical heat flux, critical mass flux or ignition temperature. It is recommended to consider multiple parameters together in evaluating its flammability. Moreover, the size of cable could change the flammability diagram, as the convection is stronger around a thinner cylindrical fuel. That is, the heating effect of a thinner cable by irradiation is weaker, while the convective heating by flame becomes greater to accelerate the flame spread. As the insulation thickness decreases, the flame spread rate will increases, while the burning duration decreases due to the reduction of fuel load.

4. Conclusions

In this work, the ignition and upward flame spread over the 1-m long cable was investigated under an axially-uniform growing heat flux, following the previous work on swelling and auto-ignition behaviors of the 0.1-m long cable sample. Results showed that the flame-retardant cables, which are normally installed in narrow closed spaces in clusters, might be easily ignited by a small flame after a weak external preheating (5 kW/m^2) to 70 ℃. As the external heat flux increases, the cable surface temperature increases, and the upward flame spread rate increase significantly. Once the cable surface reaches about 250 ℃, piloted ignition can be achieved. With the combined effect of external heating and smoldering, auto-ignition could be achieved once the cable sheath reaches 500 ℃ or the heat flux is above 18 kW/m^2.

Moreover, the burning of the flame-retardant cables might be rather intense with severe melting and dripping, as well as the swelling and cracking. The falling cracks and dripping flow can form a pool fire on the ground to increase the fire hazard. Finally, a new fire-zone diagram with only fuel characteristics (surface temperature and critical mass flux of ignition) while independent of external heating was proposed to quantify the overall fire hazard of cable. This work provides important information about the ignition and fire spread behaviors of the flame-retardant cable under a real fire scene and may guide the design of fire-resistant cables.

Acknowledgement

This work was supported by the National Key R&D Program of China (2017YFC0806400), National Natural Science Foundation of China (No. 51876183), the Fundamental Research Funds for the Central Universities (WK2320000041, WK2320000043, WK2320000047).

References

[1] Keski-Rahkonen O, Mangs J. Electrical ignition sources in nuclear power plants: Statistical, modelling and experimental studies. Nuclear Engineering and Design 2002;213:209–21. doi:10.1016/S0029-5493(01)00510-6.

[2] Huang X, Nakamura Y. A Review of Fundamental Combustion Phenomena in Wire Fires. Fire Technology 2020;56:315–60. doi:10.1007/s10694-019-00918-5.

[3] BACK KW. Methods and Methods and Methods. Contemporary Psychology: A Journal of Reviews 1976;21:20–1. doi:10.1037/014836.

[4] Campbell R. Home Electrical Fires. National Fire Protection Association (NFPA) 2019.

[5] Gallucci RHV. Statistical Characterization of Cable Electrical Failure Temperatures Due to Fire for Nuclear Power Plant Risk Applications. Fire Technology 2017;53:401–12. doi:10.1007/s10694-016-0616-0.

[6] Gong T, Xie Q, Huang X. Fire behaviors of flame-retardant cables part I: Decomposition, swelling and spontaneous ignition. Fire Safety Journal 2018;95:113–21. doi:10.1016/j.firesaf.2017.10.005.

[7] Sun P, Lin S, Huang X. Ignition of thin fuel by thermoplastic drips: An experimental study for the dripping ignition theory. Fire Safety Journal 2020;115:103006. doi:10.1016/j.firesaf.2020.103006.

[8] Xie Q, Zhang H, Ye R. Experimental study on melting and flowing behavior of thermoplastics combustion based on a new setup with a T-shape trough. Journal of Hazardous Materials 2009;166:1321–5. doi:10.1016/j.jhazmat.2008.12.057.

[9] He H, Zhang Q, Wang X, Wang F, Zhao L, Zhang Y. The Influence of Currents on the Ignition and Correlative Smoke Productions for PVC-Insulated Electrical Wires. Fire Technology 2017;53:1275–89. doi:10.1007/s10694-016-0634-y.

[10] Kikuchi M, Fujita O, Ito K, Sato A, Sakuraya T. Experimental study on flame spread over wire insulation in microgravity. Symposium (International) on Combustion 1998;27:2507–14. doi:10.1016/S0082-0784(98)80102-1.

[11] Nakamura Y, Yoshimura N, Ito H, Azumaya K, Fujita O. Flame spread over electric wire in sub-atmospheric pressure. Proceedings of the Combustion Institute 2009;32 II:2559–66. doi:10.1016/j.proci.2008.06.146.

[12] Huang X, Nakamura Y, Williams FA. Ignition-to-spread transition of externally heated electrical wire. Proceedings of the Combustion Institute 2013;34:2505–12. doi:10.1016/j.proci.2012.06.047.

[13] Kobayashi Y, Huang X, Nakaya S, Tsue M, Fernandez-Pello C. Opposed Flame Spread over Wires: the Role of Dripping and Core. Fire Safety Journal 2017;91:112–22. doi:10.1016/j.firesaf.2017.03.047.

[14] Tewarson A, Khan MM. Flame propagation for polymers in cylindrical configuration and vertical orientation. Symposium (International) on Combustion 1988;22:1231–40. doi:10.1016/S0082-0784(89)80134-1.

[15] Journeaux T, Försth M, Messa S, Kobilsek M, Sundström B, Johansson P, et al. CEMAC - CE-marking of cables. SP Rapport NV - 2010:27 2010.

[16] Huang X, Zhu H, Peng L, Zheng Z, Zeng W, Bi K, et al. Thermal Characteristics of Vertically Spreading Cable Fires in Confined Compartments. Fire Technology 2019;55:1849–75. doi:10.1007/s10694-019-00833-9.

[17] Novak C, Keller M, Meza T, McKinnies J, Espinosa E, Calhoun K. Pinched Cord and Overdriven Staple Failures: Research on the Causation of an Electrical Fire. Fire Technology 2018;54:921–41. doi:10.1007/s10694-018-0715-1.

[18] Zavaleta P, Hanouzet R, Beji T. Improved Assessment of Fire Spread over Horizontal Cable Trays Supported by Video Fire Analysis. Fire Technology 2019;55:233–55. doi:10.1007/s10694-018-0788-x.

[19] Fernandez-Pello A, Hasegawa H, Staggs K, Lipska-quinn A, Alvares N. A Study Of The Fire Performance Of Electrical Cables. Fire Safety Science 1991;3:237–47. doi:10.3801/iafss.fss.3-237.

[20] Courty L, Garo JP. External heating of electrical cables and auto-ignition investigation. Journal of Hazardous Materials 2017;321:528–36. doi:10.1016/j.jhazmat.2016.09.042.

[21] Miyamoto K, Huang X, Hashimoto N, Fujita O, Fernandez-Pello C. Limiting oxygen concentration (LOC) of burning polyethylene insulated wires under external radiation. Fire Safety Journal 2016;86:32–40. doi:10.1016/j.firesaf.2016.09.004.

[22] Torero J. Flaming Ignition of Solid Fuels. In: Hurley MJ, Gottuk DT, Hall JR, Harada K, Kuligowski ED, Puchovsky M, et al., editors. SFPE Handbook of Fire Protection Engineering. 5th ed., New York, NY: Springer; 2016, p. 633–61. doi:10.1007/978-1-4939-2565-0.

[23] Osorio AF, Mizutani K, Fernandez-Pello C, Fujita O. Microgravity flammability limits of ETFE insulated wires exposed to external radiation. Proceedings of the Combustion Institute 2015;35:2683–9. doi:10.1016/j.proci.2014.09.003.

[24] Konno Y, Kobayashi Y, Fernandez-Pello C, Hashimoto N, Nakaya S, Tsue M, et al. Opposed-Flow Flame Spread and Extinction in Electric Wires: The Effects of Gravity, External Radiant Heat Flux, and Wire Characteristics on Wire Flammability. Fire Technology 2020;56:131–48. doi:10.1007/s10694-019-00935-4.

[25] Vermesi I, Roenner N, Pironi P, Hadden RM, Rein G. Pyrolysis and ignition of a polymer by transient irradiation. Combustion and Flame 2016;163:31–41. doi:10.1016/j.combustflame.2015.08.006.

[26] Vermesi I, DiDomizio MJ, Richter F, Weckman EJ, Rein G. Pyrolysis and spontaneous ignition of wood under transient irradiation: Experiments and a-priori predictions. Fire Safety Journal 2017;91:218–25. doi:10.1016/j.firesaf.2017.03.081.

[27] Lizhong Y, Zaifu G, Yupeng Z, Weicheng F. The influence of different external heating ways on pyrolysis and spontaneous ignition of some woods. Journal of Analytical and Applied Pyrolysis 2007;78:40–5. doi:10.1016/j.jaap.2006.04.001.

[28] Gollner MJ, Huang X, Cobian J, Rangwala AS, Williams FA. Experimental study of upward flame spread of an inclined fuel surface. Proceedings of the Combustion Institute 2013;34:2531–8. doi:10.1016/j.proci.2012.06.063.

[29] Elliot PJ, Whiteley RH. Cone calorimeter test for the measurement of flammability properties of insulated wire. Polymer Degradation and Stability 1999;64:577–84. doi:10.1016/S0141-3910(98)00135-9.

[30] Rein G. Smoldering Combustion. SFPE Handbook of Fire Protection Engineering 2014;2014:581–603. doi:10.1007/978-1-4939-2565-0_19.

[31] Babrauskas V. The Cone Calorimeter. In: Hurley M, editor. SFPE Handbook of Fire Protection Engineering. 5th Editio, London: Springer; 2016, p. 952–80. doi:10.1007/978-1-4939-2565-0.

[32] Quintiere J. Radiant Panel Rate of Flame Spread Apparatus 1981.

[33] ISO 5658-2. Reaction to fire tests -- Spread of flame -- Part 2: Lateral spread on building and transport products in vertical configuration. International Organization for Standardization, Geneva 2006.